

## Test-Particle Simulation of Space Plasmas

Richard Marchand\*

*Department of Physics, University of Alberta, 11322 89 Avenue, Edmonton, Alberta, T6G 2G7, Canada.*

Received 20 October 2009; Accepted (in revised version) 28 January 2010

Communicated by Zhihong Lin

Available online 15 April 2010

---

**Abstract.** Test-particle simulations provide a useful complement to the kinetic simulations of many-body systems and their approximate treatment with multiple moments. In a kinetic approach, systems are described at a microscopic level in terms of a large number of degrees of freedom. Fluid or multiple moment approaches, however, provide a description at the macroscopic level, in terms of relatively few physical parameters involving averages or moments of particle distribution functions. Ideally, fully kinetic descriptions should be done whenever possible. Due to their complexity, the use of these approaches is often not practical in many cases of interest. In comparison, the fluid approximation is much simpler to implement and solve. It can be used to describe complex phenomena in multi-dimensional geometry with realistic boundary conditions. Its main drawback is its inability to account for many phenomena taking place on fine space or time scales, or phenomena involving nonlocal transport. Macroscopic approaches are also not adapted to describe large deviations from local equilibrium, such as the occurrence of particle beams or otherwise strong anisotropy. With the test-particle method, particle trajectories are calculated using approximated fields obtained from a low level approach, such as multiple moments. Approximate fields can also be obtained from experiments or observations. Assuming that these fields are representative of actual systems, various kinetic and statistical properties of the system can then be calculated, such as particle distribution functions and moments thereof. In this paper, the test-particle method is discussed in the context of classical statistical physics of many-body interacting point particles. Four different formulations of the method are presented, which correspond to four broad categories of the application encountered in the field of plasma physics and astronomy.

**AMS subject classifications:** 70B05, 70-01, 85-08, 65P99

**Key words:** Test-particle method, first order kinetic modelling, space plasmas.

---

\*Corresponding author. *Email address:* Richard.Marchand@ualberta.ca (R. Marchand)

## 1 Introduction

Test-particle calculations have been applied to study a broad class of problems in space physics and astronomy. The underlying assumption in these applications is that, by following the evolution of particles in fields that are deemed to be good approximations of those encountered in actual systems, useful information can be inferred concerning particle kinetics. In that sense, the test-particle approach provides a first order approximation of kinetic properties of a system, given fields obtained from a macroscopic approach or from measurements. In the absence of iterations and feedback from calculated particle trajectories, the results are generally not self-consistent. The approach is nonetheless useful for understanding several aspects of particle transport and dynamics in complex systems, in which a fully consistent kinetic calculation is not practical. This approach has been applied to many problems related to particle transport and energisation in space plasmas, and it continues to be a valuable complement to large scale simulations made with fluid codes.

In the following, four types of formulations are presented that are representative of the majority of the test-particle applications encountered in the literature. These are 1) Trajectory Sampling, 2) Forward Monte Carlo, 3) Forward Liouville and 4) Backward Liouville. In Section 3, each formulation is described in detail, and illustrated with simulation results. For consistency, and in order to clearly illustrate similarities and differences between the four approaches, each method is applied to the same physical problem: that of a perpendicular plane shock in a collisionless plasma. This particular problem was chosen for its simplicity. It is nonetheless sufficient to illustrate the use of each approach, and display their similarities and differences. In this presentation, the test-particle approach is described in the context of classical mechanics of point particles with no internal degrees of freedom. These assumptions may seem somewhat restrictive. They nonetheless encompass a broad class of near Earth plasmas and astronomical applications. In cases where these assumptions need to be relaxed; for example, with ions having different ionisation stages or electron excitation levels, some of the formalism can be readily modified to accommodate for more general conditions.

The conditions of validity of the test-particle method depend on the particular formulation considered. Given the absence of iterations between the particle and current densities inferred from a test-particle calculation, and the fields used to calculate trajectories, a general condition for validity is that these fields be sufficiently close to being self-consistent. A precise assessment of this condition is difficult to make *a priori*, as a measure of self-consistency would require a fully kinetic calculation. A first assessment of consistency can be made, for example, by comparing moments of the test-particle distribution functions with corresponding quantities such as particle densities, fluxes or current densities appearing in the macroscopic models used to approximate the fields. A further assessment can, in principle be made by computing first order corrections to the fields based on the approximate plasma distribution functions obtained in the test-particle approximation. In addition to the requirement of near consistency of the fields, two of the

approaches presented rely on one extra assumption in order to be applicable. Specifically, both the Forward Liouville and Backward Liouville approaches assume that the plasma is well described with the Vlasov equation, and that the single-particle Liouville theorem is valid. In those cases, the plasma must be nearly collisionless and processes such as charge exchange or inelastic collisions with other species should be negligible for the length and time scales of interest. It is worth noting, however, that the other two approaches considered (Trajectory Sampling and Forward Monte Carlo) are not limited by these processes. These approaches can be applied even when the evolution of distribution functions is described by a full Boltzmann equation. In this case, however, in addition to external fields, single particle trajectory calculations must account for stochastic forces corresponding, for example, to Coulomb collisions, charge exchange or inelastic collisions with neutral or ion species.

The remainder of the article is organised as follows. The physical problem considered to illustrate the four formulations of the method is described in Section 2. The four formulations of the test-particle approach are then described in Section 3. In each case, example applications are cited from published articles. The method is also illustrated by applying it to the same physical problem mentioned above. A summary and some concluding remarks are given in Section 4.

## 2 Case problem: Ideal MHD perpendicular plane shock

The solution to the ideal MHD perpendicular plane shock problem has been described elsewhere [5]. It is summarised here for completeness. In the reference frame of the shock, plasma comes toward the interface in the upstream region, and flows away from it in the downstream or shocked region. In a perpendicular shock, the magnetic field is perpendicular to the normal to the plane interface, as illustrated in Fig. 1. All physical quantities are uniform on either side of the shock front, and they vary discontinuously at the front, as prescribed by the Rankine-Hugoniot conditions. These conditions lead to a set of algebraic equations that can be solved analytically to yield

$$v_2 = \frac{\rho_1}{\rho_2} v_1 = \zeta v_1, \quad (2.1)$$

$$B_2 = \frac{1}{\zeta} B_1, \quad (2.2)$$

$$p_2 = p_1 + (1 - \zeta) \rho_1 v_1^2 - \frac{1 - \zeta^2}{\zeta^2} \frac{B_1^2}{2\mu_0}, \quad (2.3)$$

where

$$\zeta = \frac{\rho_1 v_1^2 + 4(p_1 + B_1^2/2\mu_0)}{3\rho_1 v_1^2}. \quad (2.4)$$

The electric field is calculated from the relation

$$\vec{E} = -\vec{v}_1 \times \vec{B}_1 = -\vec{v}_2 \times \vec{B}_2. \quad (2.5)$$

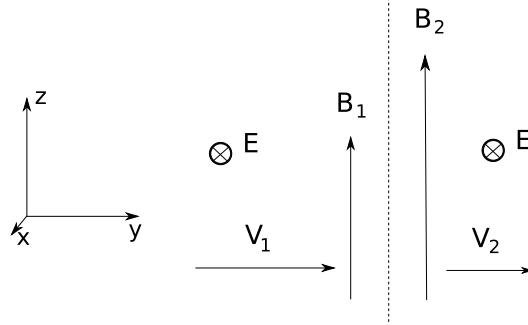


Figure 1: Illustration of the plane shock geometry in the rest frame of the shock. Flow is from left to right ( $+\hat{y}$  direction). The electric field  $E$  is pointing into the page ( $-\hat{x}$  direction), and it has the same value on either side of the shock front (dashed line). The magnetic field is in the  $+\hat{z}$  direction.

In deriving these equations, the polytropic index  $\gamma = C_P/C_V$  was assumed to be equal to two for simplicity.

Eqs. (2.2) and (2.5) constitute the macroscopic approximation to the electromagnetic fields that are used in the examples that follow. When applying the test-particle method it is necessary to integrate particle trajectories. Certain integrations schemes; e.g., simple leap frog or with explicit Runge-Kutta, only require the fields  $\vec{B}$  and  $\vec{E}$  themselves. Other schemes however; e.g., high order symplectic, are formulated in terms of the Hamiltonian and require the field potentials and their derivatives. In those cases, it is necessary to determine the scalar and vector potentials that correspond to  $\vec{B}$  and  $\vec{E}$ . For the problem considered here, those are

$$\phi_i = xv_i B_i \quad (2.6)$$

and

$$\vec{A}_i = (0, xB_i, 0), \quad (2.7)$$

where  $i = 1$  or  $2$  for the upstream or downstream region respectively. When integrating particle trajectories numerically, these expressions are actually modified so as to produce a continuous (albeit sharp) transition between the upstream (1) and downstream regions. This is obtained with

$$\phi = \frac{\phi_2 - \phi_1}{2} \tanh\left(\frac{y}{\delta}\right) + \frac{\phi_2 + \phi_1}{2} \quad (2.8)$$

and

$$\vec{A} = \frac{\vec{A}_2 - \vec{A}_1}{2} \tanh\left(\frac{y}{\delta}\right) + \frac{\vec{A}_2 + \vec{A}_1}{2}, \quad (2.9)$$

where  $\delta$  is set to one tenth the ion thermal gyroradius in the upstream region;  $\delta = \mathcal{R}_1/10$ , with

$$\mathcal{R}_1 \equiv \sqrt{\frac{2T_1}{m}} \frac{m}{qB_1}. \quad (2.10)$$

In what follows, unless stated otherwise, all coordinates are given in units of  $\mathcal{R}_1$ . The physical parameters assumed in all the examples that follow are  $n_1 = 10^6 m^{-3}$ , corre-

sponding to  $\rho_1 = n_1 \times m_p = 1.67 \times 10^{-21} \text{kg/m}^3$ ,  $T_1 = 15.65 \text{eV}$ ,  $B_1 = 4.01 \times 10^{-9} \text{T}$  and  $v_1 = 4.95 \times 10^5 \text{m/s}$ . This corresponds to a plasma with  $\beta = 0.783$ , and a magnetic Mach number  $\tilde{M} = 4.24$ , where

$$\tilde{M}^2 = v_1^2 / \left( \gamma \frac{p_1 + B_1^2 / 2\mu_0}{\rho_1} \right), \quad (2.11)$$

and

$$\beta = \frac{p_1}{B^2 / 2\mu_0} \quad (2.12)$$

is the ratio between the thermal pressure and the magnetic field pressure. With these plasma parameters in the upstream region, the factor  $\zeta$  is found to be  $\zeta = 0.371$ , which yields the value of the magnetic field in the downstream region  $B_2 = 10.82 \times 10^{-9} \text{T}$ . The electric field on either side of the shock front is  $E = 1.98 \times 10^{-3} \text{V/m}$ . In the example applications of the test-particle method considered in Section 3, the only fields required are the magnetic fields  $B_1$ ,  $B_2$ , and the electric field  $E$ .

### 3 The test-particle method – Four different approaches

Test-particle modelling has been applied to study numerous problems in space physics. While all approaches rely on the integration of particle trajectories in prescribed fields, the specifics of their formulation and use of the results may vary significantly between studies. In the following, four distinct approaches are presented, which encompass most applications of the method found in the literature. These are referred to as:

1. Trajectory Sampling,
2. Forward Monte Carlo,
3. Forward Liouville,
4. Backward Liouville.

Each formulation is distinguished by the specific kinetic aspects of the system that it focuses on, and by the underlying assumptions used in the analysis. For clarity, each approach is illustrated by applying it to the same orthogonal plane shock problem described above.

#### 3.1 Trajectory sampling

This approach consists of visualising individual particle trajectories, or groups of trajectories to provide a qualitative understanding of transport, or more generally, the kinetic properties of a system. An early application of the method was made by Speiser in a study of the penetration of Dungey's open magnetosphere by solar wind protons [11] and a possible explanation for the observed distribution of auroral particles. Buchner and Zenelyi also used this approach to study the dynamics of particles in high curvature

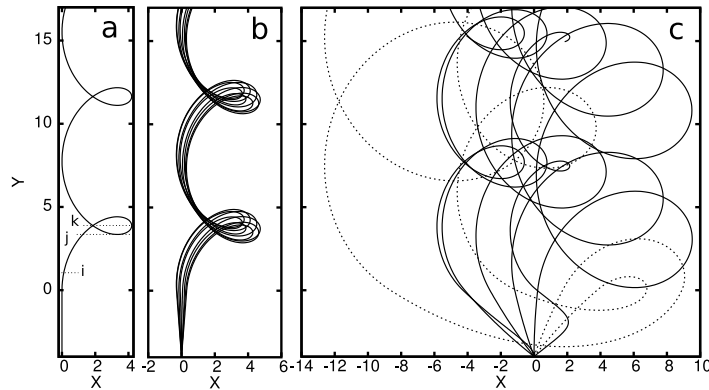


Figure 2: Illustration of trajectories for representative particles across the shock front. Panel a shows the trajectory of a particle for which the distribution function is maximum. The penetrations passed the shock front, labeled i, j and k will be referred to in a later figure. Panel b is for particles uniformly distributed in  $v_x, v_y$ , one standard deviation away from the maximum of  $f$ , in the upstream region. Similarly, panel c shows trajectories of particles distributed uniformly in  $v_x, v_y$  ten standard deviations away from the maximum. Dashed curves show trajectories with multiple crossings of the shock front. Spatial coordinates are in units of the upstream thermal gyroradius  $\mathcal{R}_1$ . The electric field is in the  $-\hat{x}$  direction.

regions of the plasma sheath, where the first adiabatic invariant breaks down [2]. Delcourt used a similar approach to study the energisation of  $O^+$  ions during the expansion phase of a substorm [3].

Similarly, Takeuchi investigated possible energisation mechanisms in expanding magnetised plasma clouds by analysing single particle trajectories in prescribed electric and magnetic fields [12].

Trajectory sampling is illustrated in Fig. 2, for the reference shock problem described above. The figure shows several representative trajectories for particles crossing the shock front. Inspection of these trajectories is useful in understanding, for example, how particles may gain or lose energy as they cross the shock front. Thermal particles; that is, particles that are near the maximum of the distribution function in the upstream region (panels a and b) are seen to have their guiding centre shifted in the direction opposite that of the electric field (to the right in the figure). As a result, those particles experience a decrease in their average kinetic energy. More energetic particles, however (panel c) have more complex trajectories. Some may cross the shock front more than once. Some may have their guiding centre shifted either to the right, corresponding to a loss of average kinetic energy, or to the left, corresponding to energisation. From this figure, periodic particle bunching can be anticipated at penetrations into the downstream region, where thermal particles slow down and turn around in their progression in  $y$ . At these locations, the ion density is expected to have local maxima.

### 3.2 Forward Monte Carlo

This approach is the most straightforward and probably the most intuitive for relating test-kinetic simulations with actual observations. It is similar to the PIC simulation ap-

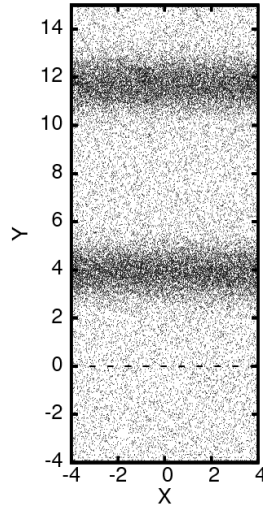


Figure 3: Density distribution resulting from a random injection of test-particles at  $y = -4\mathcal{R}_1$ . The dashed line at  $y=0$  indicates the position of the ideal MHD shock front.

proach, with the exception that the fields used to advance particle trajectories are specified *a priori*; that is, they are not calculated self consistently from moments obtained from these trajectories. A typical application involves a random injection of particles consistent with a given distribution in space and velocity in a region where this distribution is presumed to be known. Trajectories are then integrated forward in time until particles enter the regions of interest. By sampling the distribution of velocities over small volume elements, it is then possible to calculate the velocity distribution function or its moments at specific times and locations in the system. Several uses of this approach can be found in the literature. For example, the method has been used to study the penetration of the solar wind ions into the magnetosphere under northward IMF [1, 10], the generation the formation and the distribution of  $N_a$  clouds near the moon [7], the plasma sheet and ring current from solar and polar ion sources [8], auroral  $O^+$  outflow [9] and ion energisation in Mercury's ionosphere during substorms [4]. The method is illustrated in Fig. 3, with a distribution of particles in the  $x$ - $y$  plane resulting from steady injection in the upstream region. In this case, particles are injected randomly in  $x$ , and their distribution in velocity is consistent with a shifted Maxwellian

$$f(v) = n \left( \frac{m}{2\pi T} \right)^{3/2} \exp \left( -\frac{m(\vec{v} - \vec{v}_0)^2}{2T} \right), \quad (3.1)$$

where  $\vec{v}_0 = v_0 \hat{y}$  is the upstream drift velocity (in the shock frame of reference) of incoming plasma. This figure provides a good graphical representation of the density profile downstream of the shock, with the ion density being proportional to the density of points in the figure. A notable difference between this distribution and that implicit in the Hugoniot conditions is that 1) there is no discontinuous step in the density at the shock front, and 2) the density profile exhibits periodic increases in the downstream region, with the

first peak occurring approximately at  $y \simeq 4\mathcal{R}_1$  into the shock region. Comparing with Fig. 2 *a* and *b*, we see that as expected, the peaks in density coincide with the location where thermal particles turn around in their motion in  $y$ . As it stands, however, the figure contains no quantitative information. Such information, needed for example to calculate actual densities, particle fluxes and the stress tensor, can readily be obtained by attributing a statistical weight  $w_i$  to each injected particle. The weights are then used in calculating averages of the distribution function or moments thereof. The usual way to determine weights in such a calculation is to take the ratio between the physical particle flux in the injection region and that of particles injected in the simulation. Thus, for example, in the reference plane shock problem, the physical proton flux in the upstream region is  $\Gamma_{phys.} = nv_0 = 4.95 \times 10^{11} m^{-2}s^{-1}$ . If, in the simulation, the injected flux were  $\Gamma_{sim.} = 100 m^{-2}s^{-1}$ , then the weight of injected protons would be  $w_i = 4.95 \times 10^9$ . In general, the weight assigned to particles may vary depending on the time and position of injection. This would correspond to possible temporal or spatial variations in the physical flux in the injection region. Once a weight has been assigned to a particle, however, it remains constant through the entire simulation, or until the particle exits the simulation domain. The main advantage of this approach is its simplicity. It essentially duplicates nature, albeit with approximate fields and much fewer particles. Its main drawback, is that it produces large statistical errors. This is particularly true when considering the distribution function in regions of space where plasma density is low, or in regions of velocity space where  $f$  is small. Statistical errors also increase when considering high velocity moments of the distribution function, as these moments are more heavily weighted by higher energy particles of which there are relatively fewer. Thus, for example, the average density over a given volume element  $\delta V$  would be given by the sum of all the weights  $w_i$  of particles in that volume divided by  $\delta V$ . Similarly, the  $x$  component of the particle flux would be obtained from

$$\Gamma_x = \frac{1}{\delta V} \sum_{i=1}^N w_i v_{ix}, \quad (3.2)$$

where the summation is restricted to particles contained within the volume element. Similarly, the distribution function  $f$  would be computed over a small volume element by partitioning velocity space into a number of bins, and adding all the particles within the volume element and within the respective velocity bins, times the weight factors, and dividing by  $\delta V$  and by the size of the velocity bins. It should be clear from this discussion, that estimates made with this forward approach will contain large statistical errors whenever the numbers of sampled particles are not sufficiently large. These numbers can always be increased, in principle, by a) increasing the total number of particles used in a simulation, b) considering larger sampling volumes, or c) taking averages in time. Routine simulations can be made with up to  $10^9$  test-particles. For complex systems with rapid transients or short scale length structures, however, this remains a limitation. Relative statistical errors, which scale as  $1/\sqrt{N}$  where  $N$  is the number of particles involved

in the sampling, would be particularly significant in regions of velocity space where  $f$  is small, or when considering higher moments of  $f$ . In cases where a good estimate of the distribution function is needed, a variant approach can be formulated, which results in considerably lower levels of statistical errors.

### 3.3 Forward Liouville

This approach makes use of the fact that, for a collisionless plasma described by the Vlasov equation, the single particle distribution function remains constant along particle trajectories. This is the equivalent of Liouville's theorem applied to a single particle distribution function. A straightforward improvement of the method described in the previous subsection therefore consists of "tagging" each test-particle with the numerical value of  $f$  calculated in the injection region (where  $f$  is known). When sampling the distribution function in a volume element  $\delta V$ ,  $f$  is then obtained directly from the "tags" on the given particle velocities in that volume element. The result is a distribution of scattered (unstructured) points in velocity space, at which  $f$  is known exactly, without statistical errors. This approach has recently been used to model non-gyrotropic ion distributions resulting from injection in non uniform magnetic and electric fields [13]. It is otherwise less frequently encountered in the literature than the Forward Monte Carlo method described in the previous sub section. This is likely due to the fact that it is limited to collisionless plasmas for which the Liouville theorem applies. With plasmas that are well approximated by the Vlasov equation, however, the use of the method is essentially as straightforward as that of the Forward Monte Carlo method.

Results obtained with this method are presented in Fig. 4 for the plane shock problem considered in the previous paragraphs. The left panel shows a distribution of scattered points in  $v_x, v_y$  for particles sampled in the  $-10^4 m/s \leq v_z \leq 10^4 m/s$  velocity interval; i.e., for  $-0.26 \lesssim v_z/\sigma \lesssim 0.26$ . The main difference with the Forward Monte Carlo approach is that here  $f$  is not inferred from counting particles in velocity bins in a given volume element. It is therefore less affected by statistical error. Without the need for sampling in velocity space, the only statistical errors are those associated with the (random) number of particles in the sampling box in configuration space. This then provides a discretisation of the distribution function on a scattered grid in velocity, averaged over a given volume element. This, in turn, can be used to interpolate  $f$  onto a regular velocity grid, or directly calculate moments of the distribution function with reduced statistical uncertainties.

### 3.4 Back-tracking Liouville

For collisionless plasmas described by the Vlasov equation, this approach provides the most detailed description of particle kinetics without any statistical error. With the exception of numerical errors in integrating trajectories, the only errors are those resulting from the approximate fields (electromagnetic or gravitational) used to integrate particle trajectories, and in the discretisation of  $f$  in velocity. If the fields used in the integration

of trajectories had exact temporal and spatial dependences, and if trajectories could be integrated exactly, then the resulting  $f$  would also be exact. As the name suggests, the approach consists of integrating particle trajectories at a given time  $t_1$ , position  $\vec{r}_1$  and velocity  $\vec{v}_1$  backward in time until the particle reaches an input region, say at time  $t_0$ , position  $\vec{r}_0$  and velocity  $\vec{v}_0$ , where the distribution function is known. It then follows from Liouville's theorem, that the distribution function at  $\mathbf{1}$  is obtained from that at  $\mathbf{0}$  by  $f(\vec{r}_1, \vec{v}_1, t_1) = f(\vec{r}_0, \vec{v}_0, t_0)$ . The main difference between this approach and the previous one is that  $\mathbf{1}$ , the end point in phase space, is specified exactly *a priori*. It does not rely on sampling over a volume element, as in the Forward Monte Carlo or Forward Liouville approaches. It is therefore free from statistical sampling errors. This approach is particularly well suited to model regions of phase space where  $f$  is small.

An illustration of the method is given in Fig. 5 for cut planes  $v_z = 0$  of the distribution function at three penetrations into the shocked region. These penetrations correspond to  $y = 2.000$  for panel a,  $y = 3.347$  for b and  $y = 3.869$  for c. These correspond to the dashed lines marked respectively i, j and k in Fig. 2 a. As expected, the number of maxima in the distribution function coincides with the number of times a particle initially traveling at the plasma drift velocity in the upstream region, crosses the specified value of  $y$  (see Fig. 2a). It is interesting to note that panel c in Fig. 5 compares well with the distribution function sampled in  $3.9 \leq z \leq 4.0$ , in the Forward Liouville approach. The lower values of  $f$  in Fig. 2 is a consequence of finite volume sampling and of the interpolations made on the uniform velocity grid used for plotting. The occurrence of density maxima at  $y \sim 4$  and  $y \sim 12$  in Fig. 3 matches with values of  $y$  where particles traveling with the maximum of the distribution function (Fig. 2a) turn around. Fig. 5 shows that at these values of  $y$ , the distribution function is broadest in velocity space, which is consistent with the occurrence of a density maximum at those positions.

A difficulty with this approach, which is not encountered in the previous two approaches, is that in the absence of finite volume sampling, the computed distribution function can exhibit very complex structures. This is not apparent in the simple problem considered here, where  $f$  was relative smooth and nearly periodic in the  $y$  coordinate. In more complex systems, however, in the absence of symmetry or ignorable coordinates, increasingly fine structures in the distribution function can develop as one moves away from the source region. This difficulty was encountered, for example, when applying the method to assess consistency between test-kinetic simulations and an MHD model of Earth bow shock [6]. In that case, the distribution function was found to develop increasingly complex features in velocity space, as one penetrates into the downstream region. This point is illustrated in Fig. 6 with a profile of  $f$  in a velocity cut plane approximately 1.5 Earth radii into the plasma sheath region, along the sun-earth axis. In addition to the short scale structures found in velocity space, these structures also vary on short scale lengths in configuration space as one penetrates into the shocked plasma. These sharp variations in velocity and configuration space would, of course be attenuated if  $f$  were averaged over finite sampling volumes. Sampling is intrinsic in the previous approaches (Forward Monte Carlo and Forward Liouville). The strength of the Backward Liouville

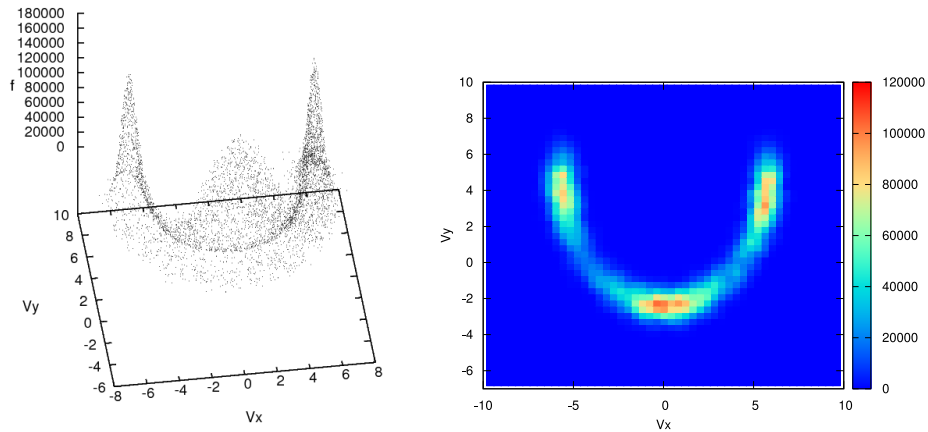


Figure 4: Distribution function sampled in the domain  $-4 \leq x \leq 4$ ,  $3.9 \leq y \leq 4$ ,  $-1 \leq z \leq 1$  in configuration space, for  $-10^4 \leq v_z \leq 10^4$ . The left panel shows a scattered plot of  $f$  as a function of particle velocities in the domain. The right panel shows colour contours of  $f$  interpolated on a structured grid. Velocities are normalised with respect to the thermal velocity  $v_{th} = \sqrt{2T/m}$  and  $f$  is multiplied by  $v_{th}^3$ .

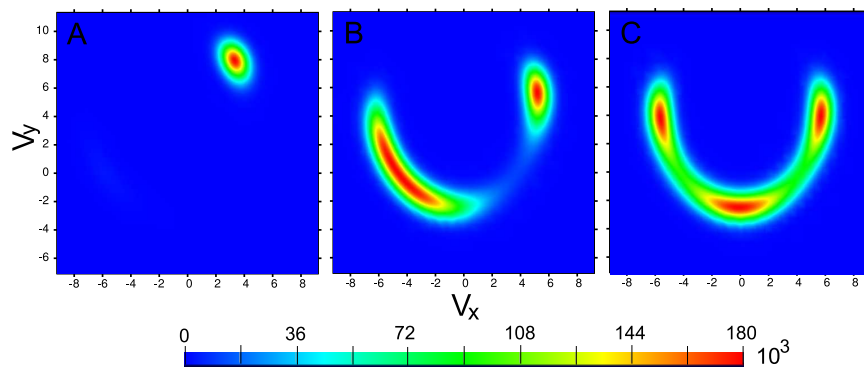


Figure 5: Colour contours of the distribution function in the  $v_z = 0$  plane at three representative positions in the downstream region. Panels a, b, c correspond to penetrations i, j and k in Fig. 2 a. Velocities are normalised with respect to the thermal velocity  $v_{th} = \sqrt{2T_1/m}$ , and the distribution function is multiplied by  $v_{th}^3$ .

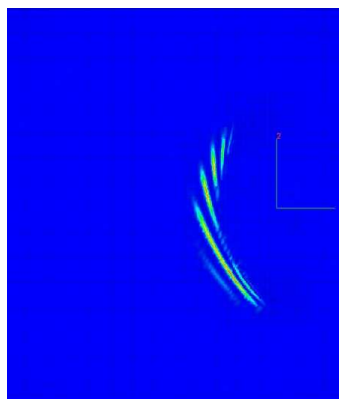


Figure 6: Cut plane illustrating fine structure in the proton distribution function in velocity space approximately 1.5 Earth radii past the bow shock into the plasma sheath, along the sun-Earth axis.

approach; its ability to produce detailed distribution functions at precise locations without statistical sampling errors, may therefore be a source of limitation. An obvious solution to this shortcoming would involve spatial averages of  $f$  using a suitable quadrature scheme. This would tend to smooth short scale variations in velocity and configuration space, while retaining an adapted representation of  $f$  without statistical noise.

## 4 Summary and conclusion

The test-particle method is used in many studies of space plasmas as a complementary approach between fluid or multiple moment models and fully kinetic models. Fluid models, such as ideal MHD, or Hall MHD are powerful tools for modelling complex systems while accounting for realistic geometry together with multiple physical processes. These models, however, are limited to the description of macroscopic properties of plasmas that can be formulated in terms of local moments of distribution functions or gradients thereof. Kinetic models, on the other hand, provide detailed information on particle dynamics, not accessible in fluid models and they are the only ones capable of describing non local transport in low collisionality plasmas. Their complexity, however, tends to limit them to relatively simple geometries and they are limited in the range of physical processes that they can account for. In that context test-particles provide a useful bridge between the two approaches. Using approximate fields obtained from macroscopic models, they can be applied to assess kinetic effects in complex systems under realistic conditions. Several formulations of the test-particle method can be made, depending on the purpose of the simulation, and the conditions of the plasma. In this review, four broad approaches are described that are believed to encompass most applications encountered in the literature. In one case, individual test-particle trajectories are considered as a tool to understand transport or energisation of particles in complex systems. In most applications, test-particle simulations are used to calculate large scale properties of systems by duplicating nature, albeit with much fewer macro-particles. The most straightforward of these approaches, the Forward Monte-Carlo method, relies on sampling test-particles in finite bins in configuration and, if needed, in velocity space. It can be applied to calculate moments of the distribution function (e.g., the density and particle fluxes), or to discretise the distribution function itself in velocity space. This approach is the one that involve the largest statistical errors, but it is also the most broadly applicable, as it doesn't rely on Liouville's theorem. In particular, it can readily be extended to include physical effects such as collisions, charge exchange, ionisation and recombination. The other two formulations presented, the Forward Liouville and the Backward Liouville approaches are less subject to statistical errors because they rely less on particle sampling over bins in configuration or velocity space. They do, however, rely on the use of Liouville's theorem for a single particle distribution function, and they are therefore only applicable to collisionless plasmas. The Backward Liouville approach is in fact free from any particle sampling and it therefore produces distribution functions that are free from statistical errors. This

method, however, suffers from its success in that, the computed distribution functions can show complex structures with short scale variations in velocity and configuration space. A solution around this difficulty would consist of averaging  $f$  in space, using a suitable quadrature scheme. In general, the choice of that scheme would be determined by the system being studied, and by the region of space considered. It would be equivalent to sampling the distribution function over finite volumes, but without statistical errors.

## Acknowledgments

This work was supported by the Natural Sciences and Engineering Council of Canada.

## References

- [1] M. Ashour-Abdalla, L.M. Zelenyi, V. Perroomian, and R.L. Richard. Consequences of magnetotail ion dynamics. *J. Geophys. Res.*, 99:14,891–916, 1994.
- [2] J. Büchner and L.M. Zelenyi. Regular and chaotic charged particle motion in magnetotail-like field reversals 1. basic theory of trapped motion. *J. Geophys. Res.*, 94:11821–42, 1989.
- [3] D.C. Delcourt. Particle acceleration by inductive electric fields in the inner magnetosphere. *J. Atmos. Sol. Terr. Phys.* 64, 551., 64:551–9, 2002.
- [4] D.C. Delcourt, F. Leblanc, K. Sekic, N. Teradad, T.E. Moore, and M.-C. Fok. Ion energization during substorms at mercury. *Planet. Space Sci.*, 55:1502–1508, 2007.
- [5] F. Mackay, R. Marchand, and K. Kabin. Test-kinetic modelling of collisionless perpendicular shocks. *J. Plasma Physics*, 74:301–18, 2008.
- [6] R. Marchand, J.Y. Lu, F. Mackay, and K. Kabin. Consistency check of a global mhd simulation using the test-kinetic approach. *Plasma Phys. Cont. Fusion*, 50:074007 1–10, 2008.
- [7] M. Mendillo, J. Emery, and Brian Flynn. Modeling the moon's extended sodium as a tool for investigating sources of transient atmospheres. *Adv. Space Res.*, 19:1577–86, 1997.
- [8] T. E. Moore, M.-C. Fok, M. O. Chandler, R. C. Chappell, S. P. Christon, D. C. Delcour, J. Fedder, M. Huddleston, M. Liemohn, W. K. Peterson, and S. Slinker. Plasma sheet and (nonstorm) ring current formation from solar and polar wind sources. *JGR*, 110:A02210, doi:10.1029/2004JA010563, 2005.
- [9] T.E. Moore, M.-C. Fok, D.C. Delcourt, S.P. Slinker, and J.A. Fedder. Global aspects of solar wind-ionosphere interactions. *J. Atmos. Sol.-Terr. Phys. (UK)*, 69(3):265–78, 2007.
- [10] R.L. Richard, R.J. Walker, and M. Ashour-Abdalla. The population of the magnetosphere by solar winds ions when the interplanetary magnetic field is northward. *Geophys. Res. Lett. (USA)*, 21:2455–8, 1994.
- [11] T.W. Speiser. Particle trajectories in a model current sheet, based on the open model of the magnetosphere, with applications to auroral particles. *J. Geophys. Res.*, 70:1717–28, 1965.
- [12] S. Takeuchi. New particle accelerations by magnetized plasma shock waves. *Phys. Plasmas*, 12:102901–6, 2005.
- [13] G. Voitcu. Private communication, 2009.